

Emmanouil S. Brilakis, Subhash Banerjee, Zhihua He,
Stephen T. Sum, Sean Madden, and James Muller

Near-infrared spectroscopy (NIRS) is a novel coronary imaging technology that analyzes the light reflected in a range of wavelengths to determine the chemical composition of tissue, including lipids such as cholesterol and cholesteryl esters. This chapter presents the basic principles of NIRS, describes the equipment and interpretation of NIRS findings, presents the studies that validated the ability of NIRS to detect lipid core plaques (LCPs), and discusses its clinical and research applications.

Principles of Diffuse Reflectance NIRS

In diffuse reflectance NIRS, light from the near-infrared region of the electromagnetic spectrum (approximately 800–2,500 nm) is directed to a sample and the diffusely reflected light is collected. The proportion of light returned from the sample is dependent on wavelength and is dependent

on loss of light in the tissue due to scattering and absorption. Scattering occurs when light is randomly reflected by cellular and extracellular structures in the sample, while absorption results from the transformation of light into molecular energy primarily in the form of molecular vibrations of atoms about their chemical bonds.

NIRS allows direct and rapid measurements for qualitative and quantitative compositional analysis in an array of applications with little to no sample preparation. As a result, NIRS has been widely adopted in many different areas including agriculture, food, petroleum, astronomy, pharmaceuticals, and medicine [1, 2].

Interpretation of the NIRS spectra of complex, multi-constituent samples is difficult and requires multivariate methods of analysis. This is accomplished by mathematical modeling using calibration samples whose chemical and physical properties span the expected range of future samples. Reference values for the target components in these samples are obtained by an independent method (e.g., histology). Models constructed from the calibration samples compare the measured NIRS signals with the reference values, allowing qualitative or quantitative determination of unknown samples based on their NIRS spectra [3].

E.S. Brilakis, MD, PhD (✉) • S. Banerjee, MD
Department of Cardiovascular Diseases,
VA North Texas Health Care System,
University of Texas Southwestern Medical School,
4500 S. Lancaster Road (111A), Dallas,
TX 75216, USA
e-mail: esbrilakis@gmail.com; subhash.banerjee@va.gov

Z. He, PhD • S.T. Sum, PhD • S. Madden, PhD,
J. Muller, MD
Infraredx, Inc., 34 Third Ave.,
Burlington, MA 01803, USA
e-mail: vhe@infraredx.com; ssum@infraredx.com;
smadden@infraredx.com; jmuller@infraredx.com

Validation of LCP Detection by NIRS

Early studies demonstrated that NIRS can detect cholesterol and collagen in rabbit and human aortic tissue and in human carotid and coronary tissue

ex vivo [4–6]. Subsequently, NIRS intravascular diagnostic systems were developed to detect lipid-rich plaque through blood [7–10].

The detection of LCP by NIRS was validated in a large study of human coronary autopsy specimens [11]. Arterial segments were first scanned during pulsatile coronary artery perfusion using blood and then cut into 2-mm thick cross-sectional blocks for histopathological analysis. A total of 84 autopsy hearts and 216 segments were used to build and validate an algorithm capable of automatically recognizing the NIRS spectral signals associated with LCP. For the purpose of this study, LCP was defined as a fibroatheroma containing a necrotic core at least 200 μm thick with a circumferential span of at least 60° on cross-section. The primary endpoint of the algorithm validation was the accuracy of detecting LCP meeting this definition. The algorithm was prospectively validated for detection of LCP in nearly 2,000 individual blocks from 51 hearts achieving an area under the receiver operating characteristic (ROC) curve (AUC) of 0.80 for lumen diameters of up to 3.0 mm.

A concurrent in vivo study called SPECTroscopic Assessment of Coronary Lipid (SPECTACL) showed prospectively that the spectral features of coronary arteries in patients were similar to those obtained from autopsy specimens [12]. The spectral similarity between NIRS measurements collected in vivo and ex vivo demonstrated the applicability of the autopsy tissue-based LCP detection algorithm to patients.

Design of the Near-Infrared: Intravascular Ultrasound Combination System and Interpretation of its Findings

Currently coronary NIRS is available as a combined NIRS and intravascular ultrasound (IVUS) system (TVC Imaging System, InfraReDx, Inc., Burlington, MA) [13]. The system consists of a console, a pullback and rotation device (PBR), and an intravascular catheter [14] (Fig. 10.1). The system console contains a near-infrared scanning laser, computer, power system, and two monitors.



Fig. 10.1 TVC imaging system, which is a combination NIRS and IVUS system. (a) The console includes two touch-screen monitors displaying the NIRS chemogram and IVUS images (transverse and longitudinal). (b) The catheter contains fiber optics and mirrors for near-infrared light, as well as a coax cable and a transducer for ultrasound

The PBR houses the electronic, optical and mechanical components for delivering and detecting ultrasound and near-infrared light signals, and for translating and rotating the imaging core of the catheter. The catheter is 3.2-Fr, rapid exchange catheter consisting of a tip with a 40 MHz ultrasound transducer and two mirrors, a core with two optical fibers and a coax cable inside a drive cable. The delivery and collection

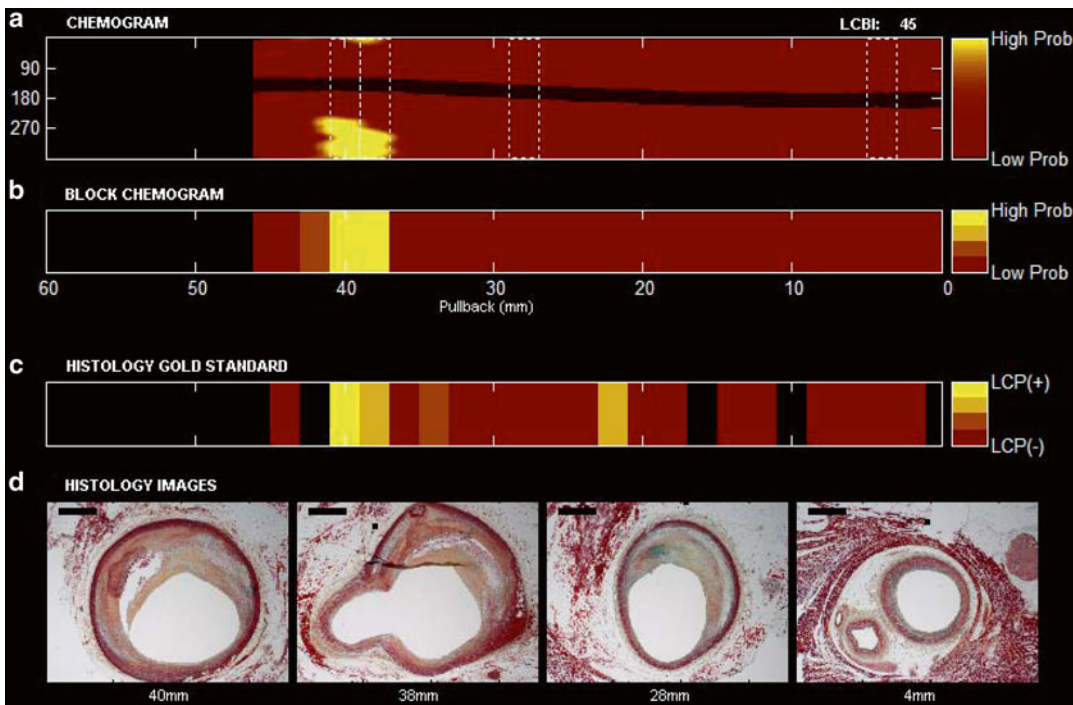


Fig. 10.2 NIRS pullback and selected histologic findings from a human coronary artery segment. **(a)** Chemogram image indicating LCP content by NIRS (x-axis=pullback distance in mm, y-axis=rotation angle in degrees). Pixel colors range from red for low probability to yellow for high probability of LCP. The contiguous black region is the guide wire. **(b)** Block chemogram image indicating summary metric of the presence of LCP at 2-mm intervals in

four probability categories. **(c)** Diagram demonstrating the presence of LCP by histologic evaluation. **(d)** Movat cross-sections from locations along the artery indicated by dotted boxes in the chemogram. *Image interpretation:* The chemogram shows large LCP signals from 36 to 42 mm. The block chemogram indicates that there is the region of the strongest signal. Histology (panel c and d) confirms the presence of fibroatheroma at this location

fibers in the core are terminated by mirrors embedded in the tip for sending incident light through blood onto the artery wall and collecting the diffusely reflected light. The coax cable transmits and receives the electrical signal to and from the ultrasound transducer. The catheter imaging core rotates at 960 rpm with automated pullback at a rate of 0.5 mm/s, interrogating tissue in a helical pattern.

In the NIRS modality, the resulting spectra are processed and interpreted by the LCP detection algorithm to generate a longitudinal image (called a chemogram) of the scanned artery segment (Fig. 10.2). Each spectral measurement is assigned a probability of LCP by the detection algorithm and displayed in a false color map (Fig. 10.3) with colors ranging from red (low probability of LCP) to yellow (high probability of LCP). From the che-

mogrom, a summary metric of the probability that an LCP is present in a 2-mm interval of the pullback is computed and displayed in a supplementary false color map called a block chemogram (Fig. 10.2b). Blocks correspond to one of four discrete categories, each represented by a distinct color (red, orange, tan, and yellow, in increasing order of LCP probability).

An additional metric, the lipid core burden index (LCBI), is used to quantify the amount of LCP in a scanned artery segment. The LCBI is defined as the fraction of yellow pixels in the chemogram multiplied by 1,000 (0–1,000 scale). Figure 10.3 illustrates the computation of the LCBI.

The transverse IVUS image is overlaid with a chemogram ring taken from the corresponding longitudinal location in the chemogram, and the

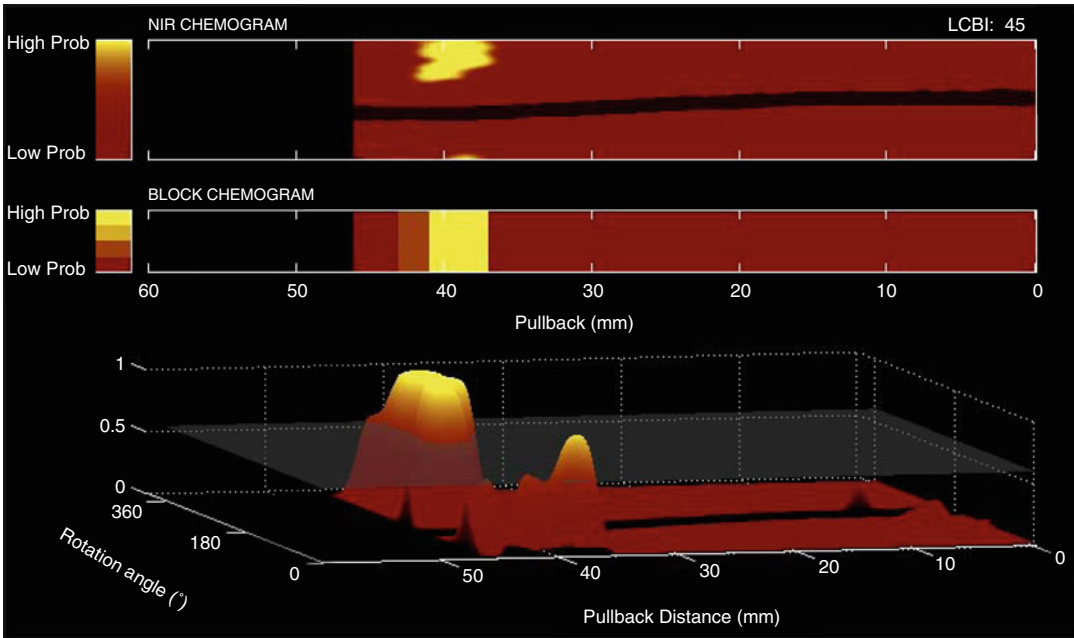


Fig. 10.3 Illustration of the lipid core burden index (LCBI). The LCBI (*top right*) shows the proportion of lipid in a scanned artery on a 0–1,000 scale. The LCBI is calculated as the fraction of valid pixels in the chemogram

that are *yellow*, multiplied by a factor of 1,000. *Yellow* pixels are those whose values (probability of LCP) exceed a specified threshold, as indicated by the horizontal plane in the *bottom panel*

block chemogram color is displayed in the catheter artifact. In addition, the longitudinal IVUS image is aligned with the chemogram and block chemogram.

ment, and (3) evaluating novel anti-atherosclerotic therapies. All these applications are currently undergoing extensive clinical evaluation.

Research and Clinical Utility of the NIRS and IVUS Catheter

In April 2008, the US Food and Drug Administration (FDA) cleared coronary NIRS for clinical use in the USA [15]. The clearance was based on the autopsy validation data [11] and the demonstration of similarity between clinical and autopsy spectra [12]. NIRS was approved for the detection of lipid core containing plaques of interest and the assessment of lipid core burden in coronary arteries. In June 2010 the FDA approved the combination NIRS-IVUS catheter.

Potential clinical applications of NIRS include: (1) improving the safety of percutaneous coronary interventions (PCIs), (2) identifying coronary lesions at risk for causing subsequent clinical events and selecting an optimal medical manage-

PCI Outcome Optimization

In spite of the rapid evolution of PCI techniques, complications such as peri-procedural myocardial infarction (MI) [16] distal embolization and acute stent thrombosis [17] continue to occur. NIRS imaging can improve the safety of PCI by enabling rapid, easy, and accurate prediction of the risk of peri-procedural complications, such as no-reflow and peri-procedural acute myocardial infarction and, as a result, providing guidance for the use of clinical measures to prevent such complications.

NIRS for Predicting Peri-procedural Myocardial Infarction

PCI of a large LCP, as detected by NIRS, has been associated with high risk for distal embolization, no-reflow, and post-PCI myocardial infarction [18–23]. Four published case reports and two case

Table 10.1 Published studies evaluating the association between NIRS findings and post-percutaneous coronary intervention myocardial infarction and no-reflow

Author	Year	<i>n</i>	Near-infrared spectroscopy finding	Outcomes
Case reports				
Goldstein et al. [18]	2009	4	Large LCP by NIRS was found in 3 cases	No-reflow occurred in two cases—one case was an autopsy case in which thrombus was formed at LCP site
Saeed et al. [19]	2010	1	Large circumferential LCP	Slow flow post-LAD stenting
Schultz et al. [20]	2010	1	Large, near-circumferential LCP	Transient chest discomfort post-stenting and post-PCI MI
Fernandez-Friera et al. [23]	2010	1	Large circumferential LCP	PCI complicated by transient no-reflow and a periprocedural MI (peak troponin, 8.1 ng/mL)
Case series				
Raghunathan et al. [21]	2011	30	Two or more yellow blocks on block chemogram	Several thresholds were used (CK-MB increase >1×, 2×, and 3× ULN)
Goldstein et al. [22]	2011	62	maxLCBI4 mm ≥500	CK-MB or troponin increase >3× ULN

LCP lipid core plaque, NIRS near-infrared spectroscopy, LAD left anterior descending artery, PCI percutaneous coronary intervention, MI myocardial infarction, LCBI lipid core burden index, CK-MB creatine kinase MB fraction, ULN upper limit of normal

series have described an association of large LCP by NIRS with no-reflow and with post-PCI myocardial infarction (MI) (Table 10.1). Goldstein et al. [18], Saeed et al. [19], and Fernandez-Friera et al. [23] presented case reports of no-reflow, whereas Schultz et al. [20] presented a case of transient chest pain and post-PCI MI after stenting of lesions containing large LCPs.

Raghunathan et al. evaluated the association between the presence and extent of coronary LCPs detected by NIRS performed prior to PCI with post-procedural myocardial infarction [21] using various LCP and MI definitions. Compared to patients who did not have post-PCI MI, those who experienced post-PCI MI had similar clinical characteristics but received more stents and had more yellow blocks within the stented lesion. CK-MB level elevation >3× the upper limit of normal was observed in 27 % of patients with two or more yellow block vs. in none of the patients with 0–1 yellow blocks within the stented lesion ($p=0.02$).

Goldstein et al. studied 62 patients undergoing PCI from the COLOR registry [22]. The extent of LCP in the treatment zone was calculated as the maximal LCBI measured by NIRS for each of the

4-mm longitudinal segments in the treatment zone. Peri-procedural MI occurred in nine patients (14.5 %). Seven of 14 patients (50 %) with a maxLCBI4mm of ≥500 had post-PCI MI compared to 2 of 48 patients (4.2 %) with maxLCBI4mm <500 ($p=0.0002$).

Several other studies using various intracoronary imaging modalities have demonstrated that the presence of LCP (thin-cap fibroatheroma, as assessed by OCT [24], necrotic core, as assessed by IVUS-VH [25], and attenuated plaque [26], as assessed by IVUS) are associated with higher incidence of no-reflow and post-PCI MI. Therefore, LCP-containing lesions are at increased risk for causing complications and could form the target for preventive and therapeutic interventions. Although patients with acute coronary syndromes are more likely to have LCPs, approximately half of patients with stable angina also had LCPs [27] within their culprit lesions, suggesting that some stable angina patients may also be at increased risk for post-PCI complications.

Whether NIRS can help identify saphenous vein graft (SVG) lesions at high risk of distal

embolization is under investigation; however, Wood et al. recently demonstrated that ostial SVG lesions were less likely to have LCPs, as detected by NIRS, compared to body lesions [28]. This lower frequency of LCP in the ostial and anastomotic lesions might explain the lower likelihood of post-PCI myocardial infarction in these lesions compared to SVG body lesions [29, 30].

NIRS-Based Insights into the Mechanism of Peri-procedural Myocardial Infarction

Whether distal embolization, thrombosis, or side-branch occlusion is the main cause of post-PCI MI remains under evaluation. Selvanayagam et al. described two patterns of myocardial injury post-PCI: one adjacent to the area of stent, presumably due to epicardial side branch occlusion and one involving the distal myocardial segment supplied by the target coronary artery, likely due to distal embolization [31].

Two pilot NIRS-based studies have provided insights on the mechanism of post-PCI MI. In the first study, an embolic protection device (EPD) was used in nine patients with large LCPs undergoing PCI [32] (Fig. 10.4). EPD use resulted in capture of embolized material in eight of the nine lesions: the captured material mainly consisted of fibrin and platelet aggregates, suggesting that a major mechanism of peri-stenting infarction might be distal embolization of thrombi associated with exposure of blood to LCP in the lesion. Post-PCI MI occurred in two patients (22%), in one of whom two filters were required because of significant debris distal embolization causing “clogging” of the filter. The role of distal embolization in post-PCI MI is further supported by several studies showing a significant decrease in LCBI post-stenting [32, 33].

Papayannis et al. extended the above observation by describing that stenting of large LCPs (defined as at least three 2-mm yellow blocks on the NIRS block chemogram with $>200^\circ$ angular extent) was more likely to lead to in-stent thrombus formation (as detected by optical coherence tomography) compared to stenting coronary lesions without large LCP [34]. Two of three

patients with a large LCP (67%) developed intrastent thrombus post-stent implantation (Fig. 10.5) compared to none of six patients without large LCPs (0%, $p=0.02$). This may be due to the high thrombogenicity of the lipid core with direct activation of platelets by the oxidized lipids, but also to the high content of active tissue factor in the lipid core, that can trigger the extrinsic clotting cascade [35]. As noted above, it is possible that the thrombus formed within the stent subsequently embolizes and EPD use may prevent embolization not only of the LCP but also of the platelet or fibrin thrombus. Interestingly, similar observations were made in an intravascular imaging study that used optical coherence tomography: Porto et al. analyzed 50 patients undergoing PCI and found three predictors of post-PCI MI: thin-cap fibroatheroma (OR 29.7, 95% CI 1.4–32.1), intrastent thrombus (OR 5.5, 95% CI 1.2–24.9), and intrastent dissection (OR 5.3, 95% CI 1.2–24.3) [24].

Given the above observations, although the optimal strategy for preventing post-PCI MI in high-risk lesions remains to be determined, it is likely that a combination strategy of an EPD and aggressive antiplatelet/anticoagulant therapy may be needed to prevent both distal embolization and the accelerated formation of intrastent thrombus that could subsequently embolize.

Several ongoing studies are evaluating the mechanism of post-PCI MI and potential preventive strategies. The Lipid Core Shift Study (NCT00905671) is examining whether PCI of large LCP lesions may cause plaque shift and side branch occlusion. The CANARY (Coronary Assessment by Near-infrared of Atherosclerotic Rupture-prone Yellow, NCT01268319) trial is a prospective randomized-controlled trial that is randomizing patients with large LCPs in native coronary arteries undergoing clinically indicated PCI to use a Filterwire (Boston Scientific, Natick, MA) or standard of care without EPD. The use of EPDs is currently only approved in the USA for SVG lesions [36].

NIRS and Stent Length Selection

Stenting from “normal” proximal to “normal” distal reference segment is usually performed

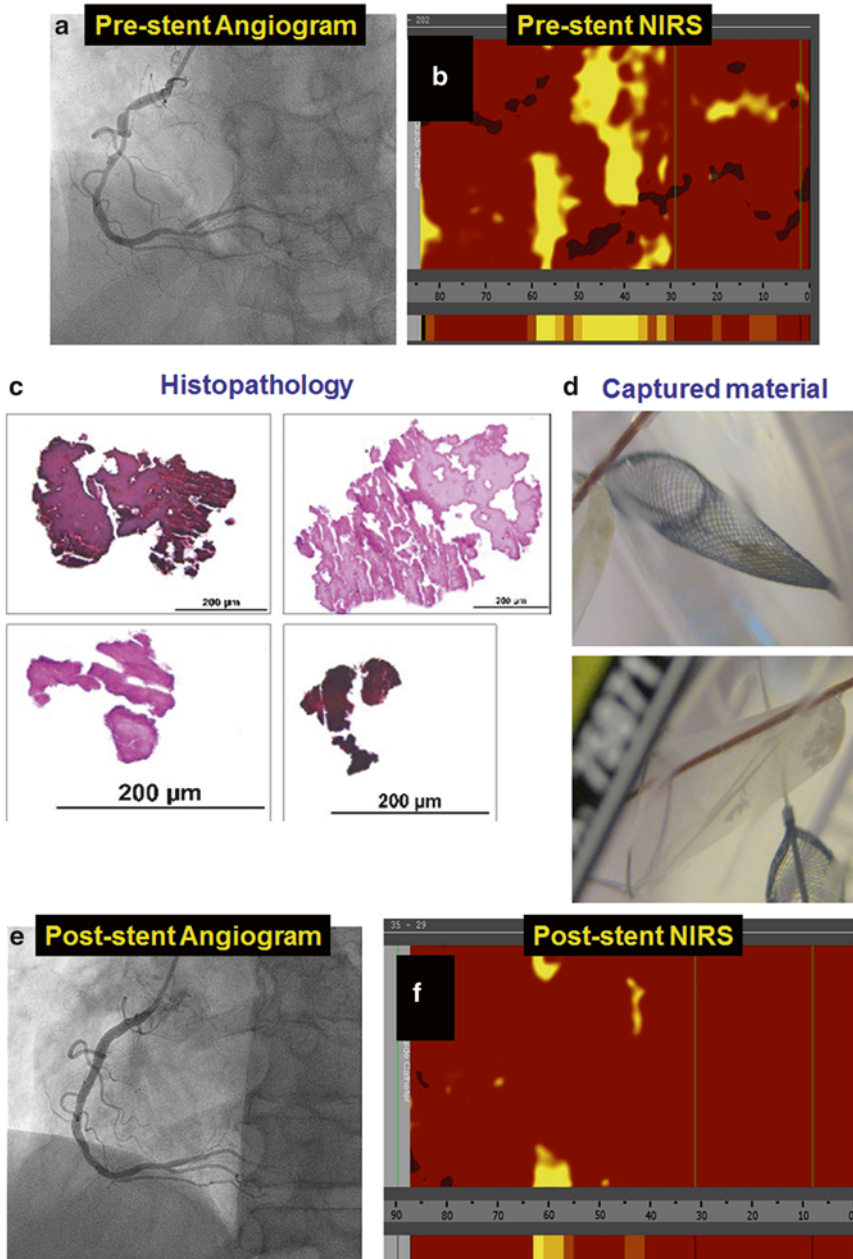


Fig. 10.4 Example of distal embolization and thrombus formation in a patient undergoing percutaneous coronary intervention. Coronary angiography demonstrating diffuse right coronary artery obstructive disease (panel **a**) with large lipid core plaque (LCP) by near-infrared spectroscopy

(panel **b**). Stenting of the right coronary artery was performed using a filter for embolic protection. Fibrin and platelet aggregates (panel **c**) were retrieved in the filter (panel **d**) post-PCI. An excellent angiographic result as obtained (panel **e**) along with reduction of the LCP size (panel **f**)

when drug-eluting stents (DES) are used for PCI. However, occasionally these angiographically “normal” sites may contain LCP that does not narrow the lumen due to positive remodeling.

Dixon et al. analyzed 50 LCP-containing lesions and found that in eight of those lesions (16 %) LCP extended beyond the angiographic margins of the lesion [37].

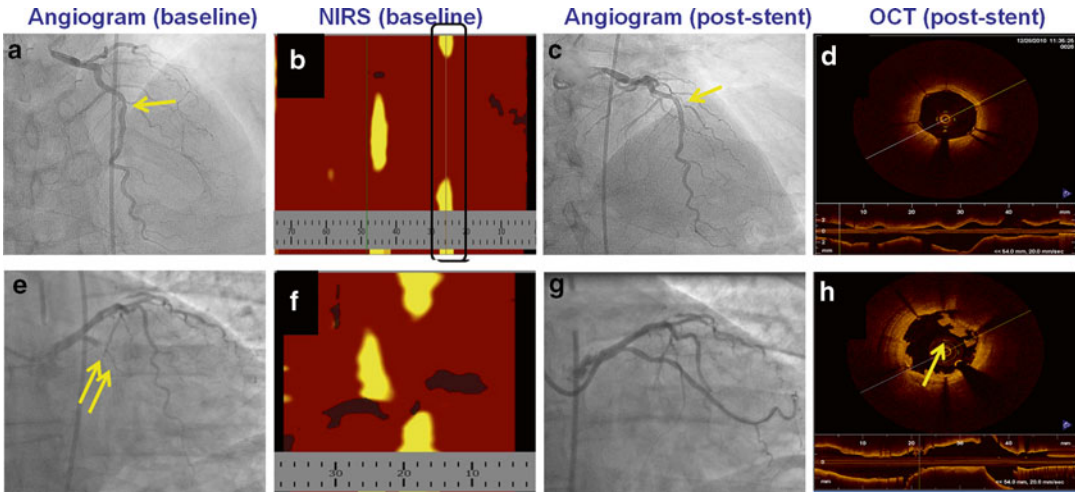


Fig. 10.5 Example of in-stent thrombus formation post-stenting of a large LCP. A patient underwent stenting of a lesion in the mid left anterior descending artery that contained a small LCP (panel b) with an excellent angiographic result (panel c) and no in-stent thrombus formation

(panel d). Another patient underwent stenting of a circumflex lesion (panel e) that contained a large LCP (panel f), and although a good angiographic result was achieved (panel g) intrastent thrombus formed post-deployment (panel h)

Disruption or incomplete coverage of such lesions might result in stent thrombosis or restenosis [38, 39]. Sakhuja et al. reported acute stent thrombosis in a patient who underwent right coronary stenting, in whom a large LCP extended proximal to the proximal stent edge [39]. Use of coronary NIRS could, therefore, aid selection of the appropriate length of artery to stent based on the length of the lesion as determined by angiography and NIR and the presence or absence of adjacent LCP.

Identification of High-Risk Coronary Lesions and Optimization of Medical Management

The identification of non-obstructive coronary lesions that are at high risk for causing subsequent adverse clinical events and demonstrating that early treatment improves clinical outcomes remains an important goal of plaque imaging [40–42]. The only group of intermediate lesions in which prophylactic stenting has been shown to be beneficial is SVG lesions. In the VELETI (Moderate VEin Graft LEsion Stenting With the Taxus Stent and IVUS) trial prophylactic stenting

of intermediate SVG lesions with a paclitaxel-eluting stent improved outcomes compared to medical therapy alone [43].

The largest natural history study of non-obstructive native coronary artery lesions is the Providing Regional Observations to Study Predictors of Events in the Coronary Tree (PROSPECT) study [36]. PROSPECT followed 697 patients with acute coronary syndromes who underwent three-vessel coronary angiography and gray-scale and radiofrequency intravascular ultrasonographic imaging after PCI of the culprit lesion [44]. After a median follow-up time of 3.4 years, the rate of major adverse cardiovascular events due to initially untreated lesions was 11.6%. Most of those lesions were either thin-cap fibroatheromas, as determined by virtual histology IVUS (VH-IVUS) or were characterized by a large plaque burden, a small luminal area, or some combination of these characteristics, as determined by gray-scale and radiofrequency intravascular ultrasonography [44]. Only 17.2% of the highest risk lesions caused symptoms during follow-up, making preemptive lesion treatment impractical.

Although theoretically attractive, whether NIRS-based LCP detection may provide better

prediction of future cardiovascular events compared to gray-scale and radiofrequency IVUS remains to be determined [45]. Brugaletta et al. demonstrated that the presence and extent of necrotic core by NIRS has only a weak association with percent necrotic core, as detected by radiofrequency IVUS [46]. Pu et al. demonstrated a weak positive relationship between radiofrequency ultrasound detected percent necrotic core and NIRS-derived LCBI in selected sets of very large non-calcified plaques, but not in calcified plaques [26]. In early analyses from the COLOR registry moderate lesions without LCP were unlikely to progress. NIRS may provide prognostic information that is not provided by traditional cardiovascular risk score systems: no correlation was found between the Framingham risk score and LCBI of a non-culprit coronary vessel among 208 patients undergoing PCI [47]. Similarly, no correlation was found between LCBI and creatinine clearance [48] and with the SYNTAX score [49].

Apart from mechanical treatments, patients with extensive LCPs might benefit from aggressive pharmacologic therapies, such as intensive antithrombotic regimen, aggressive low-density lipoprotein cholesterol lowering, high-density lipoprotein infusion, low-density lipoprotein apheresis, or with medications such as niacin, fibrates, or in the future with novel compounds that are currently under clinical trial evaluation [50]. The NIRS-IVUS coronary imaging could also serve as a marker of high coronary risk that could motivate patients to comply with the prescribed medical treatments and to adopt beneficial lifestyle changes.

Evaluation of Novel Anti-atherosclerotic Treatments

Most past and ongoing studies utilizing intracoronary imaging to assess changes in the coronary artery as a result of various treatments have used as primary endpoint the change in volume of a mildly or moderately diseased segment of the coronary artery wall (usually measured by IVUS

as percent or total atheroma volume) [51]. However, many anti-atherosclerotic therapies, especially those that target serum lipoproteins, would be more likely to affect LCP—rather than non-LCP-containing lesions. Hence, use of NIRS would be expected to provide a more sensitive endpoint in plaque regression studies. Use of NIRS in longitudinal studies is feasible given its excellent intra- and inter-catheter reproducibility [33, 52].

To date, only one study has utilized NIRS to longitudinally assess coronary lesions, the Reduction in YELlow Plaque by Aggressive Lipid-LOWering Therapy (YELLOW) Trial (presented at the 2012 American College of Cardiology annual scientific sessions in Chicago, Illinois). The YELLOW trial randomized 87 patients with multivessel coronary artery disease who were scheduled to undergo staged PCI. During the initial catheterization, all patients underwent FFR, IVUS, and NIRS of the nontarget lesion and if the lesion was hemodynamically significant (as assessed by fractional flow reserve) they were randomized to standard of care vs. rosuvastatin 40 mg daily for 6–8 weeks. They then underwent repeat coronary angiography and imaging of the nontarget lesion. In spite of the limited duration of treatment, a significant reduction in the lesion LCBI was observed (Fig. 10.6).

The Atherosclerosis Lesion Progression Intervention using Niacin Extended Release in Saphenous Vein Grafts (ALPINE-SVG) Pilot Trial is using imaging with IVUS, NIRS-IVUS, and optical coherence tomography to assess the impact of extended-release niacin in intermediate SVG lesions treated for 12 months (NCT01221402). Similarly, the Prasugrel for Prevention of Early Saphenous Vein Graft Thrombosis study (NCT01560780) is assessing the effect of prasugrel within the first year after coronary bypass graft surgery in SVGs using imaging with IVUS, NIRS-IVUS, and optical coherence tomography. Several other prospective coronary atherosclerosis studies are currently utilizing coronary NIRS as an endpoint, such as the AtheroREMO and the IBIS-3 trial. Finally, COLOR (Chemometric Observations of Lipid Core Containing Plaques of Interest in

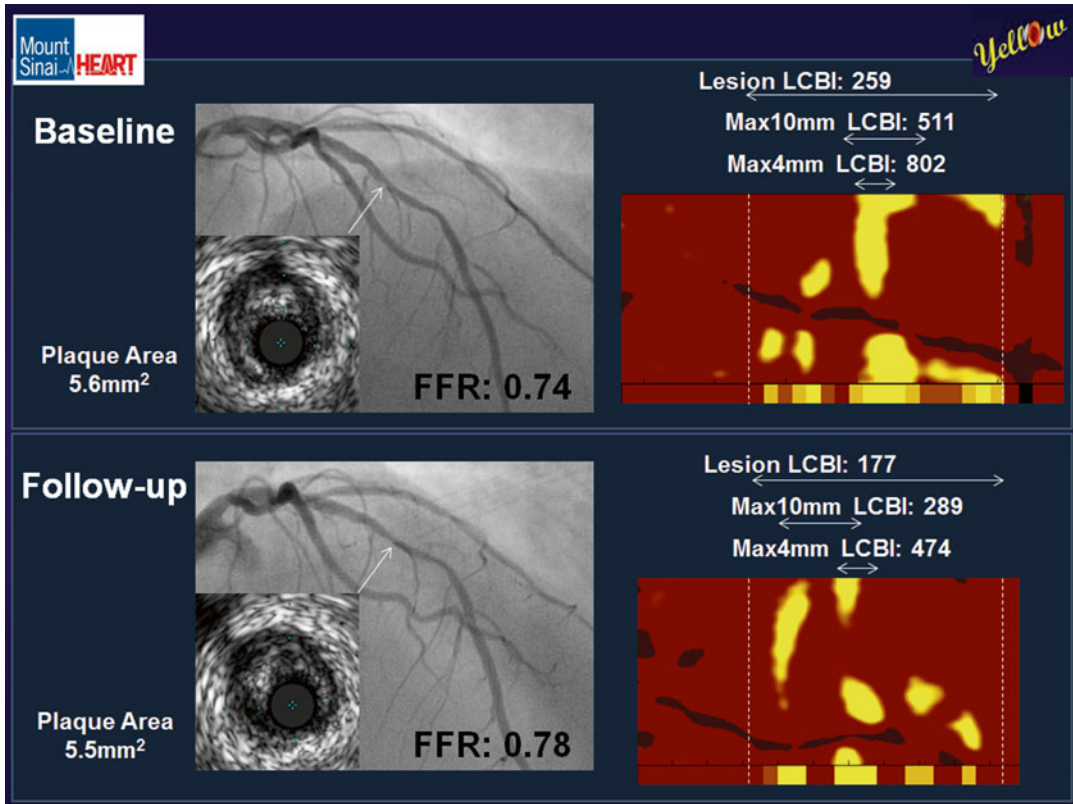


Fig. 10.6 Example of LCP regression after 2 months of intensive lipid-lowering therapy (rosuvastatin 40 mg daily) from a patient participating in the YELLOW trial

(Courtesy of Dr. Anapoorna Kini and Dr. Samin Sharma (Mount Sinai School of Medicine, New York, NY))

Native Coronary Arteries, NCT00831116) is an ongoing observational registry of coronary NIRS use in the USA that is providing valuable insights on the clinical use and utility of NIRS [22]. Over 1,100 patients are currently under observation in COLOR.

In summary, coronary NIRS is novel imaging modality for the *in vivo* detection of LCPs. It has undergone extensive development and validation and is currently being utilized to assist with clinical decision making in the cardiac catheterization laboratory and with evaluation of novel anti-atherosclerotic treatments.

Conflicts of interest: Z.H., S.T.S., S.P.M., and J.E.M. are employees of InfraReDx, Inc.

References

1. Williams P, Norris K. Near-infrared technology in the agriculture and food industries. St. Paul, MN: American Association of Cereal Chemists; 2001.
2. Ciurczak EW, Drennen JK. Pharmaceutical and medical applications of near-infrared spectroscopy. New York, NY: Marcel Dekker; 2002.
3. Lavine B, Workman J. Chemometrics. Anal Chem. 2008;80:4519–31.
4. Lodder RA, Cassis L, Ciurczak EW. Arterial analysis with a novel near-IR fiber-optic probe. Spectroscopy. 1990;5:12–7.
5. Lilledahl MB, Haugen OA, Barkost M, Svaasand LO. Reflection spectroscopy of atherosclerotic plaque. J Biomed Opt. 2006;11:021005.
6. Dempsey RJ, Davis DG, Buice RG, Lodder RA. Biological and medical applications of near-infrared spectrometry. Appl Spectrosc. 1996;50:18A–34A.

7. Marshik B, Tan H, Tang J. Discrimination of lipid-rich plaques in human aorta specimens with NIR spectroscopy through whole blood. *Am J Cardiol.* 2002;90(Suppl 6A):129H.
8. Marshik B, Tan H, Tang J. Detection of thin-capped fibroatheromas in human aorta tissue with near infrared spectroscopy through blood. *J Am Coll Cardiol.* 2003;41(Suppl 1).
9. Waxman S, Tang J, Marshik BJ. In vivo detection of a coronary artificial target with a near infrared spectroscopy catheter. *Am J Cardiol.* 2004;94(Suppl 6A):141E.
10. Caplan JD, Waxman S, Nesto RW, Muller JE. Near-infrared spectroscopy for the detection of vulnerable coronary artery plaques. *J Am Coll Cardiol.* 2006;47:C92-6.
11. Gardner CM, Tan H, Hull EL, et al. Detection of lipid core coronary plaques in autopsy specimens with a novel catheter-based near-infrared spectroscopy system. *JACC Cardiovasc Imaging.* 2008;1:638-48.
12. Waxman S, Dixon SR, L'Allier P, et al. In vivo validation of a catheter-based near-infrared spectroscopy system for detection of lipid core coronary plaques: initial results of the SPECTACL study. *JACC Cardiovasc Imaging.* 2009;2:858-68.
13. Madder RD, Steinberg DH, Anderson RD. Multimodality direct coronary imaging with combined near-infrared spectroscopy and intravascular ultrasound: initial US experience. *Catheter Cardiovasc Interv.* 2013;81(3):551-7.
14. Garg S, Serruys PW, van der Ent M, et al. First use in patients of a combined near infra-red spectroscopy and intra-vascular ultrasound catheter to identify composition and structure of coronary plaque. *EuroIntervention.* 2010;5:755-6.
15. U.S. Food and Drug Administration. Coronary artery plaque imaging device cleared by FDA. Press Announcements. 29 April 2008. <http://www.fda.gov/NewsEvents/Newsroom/PressAnnouncements/2008/ucm116888.htm>. Accessed 8 July 2013.
16. Prasad A, Herrmann J. Myocardial infarction due to percutaneous coronary intervention. *N Engl J Med.* 2011;364:453-64.
17. Prasad A, Rihal CS, Lennon RJ, Wiste HJ, Singh M, Holmes Jr DR. Trends in outcomes after percutaneous coronary intervention for chronic total occlusions: a 25-year experience from the Mayo Clinic. *J Am Coll Cardiol.* 2007;49:1611-8.
18. Goldstein JA, Grines C, Fischell T, et al. Coronary embolization following balloon dilation of lipid-core plaques. *JACC Cardiovasc Imaging.* 2009;2:1420-4.
19. Saeed B, Banerjee S, Brilakis ES. Slow flow after stenting of a coronary lesion with a large lipid core plaque detected by near-infrared spectroscopy. *EuroIntervention.* 2010;6:545.
20. Schultz C, Serruys P, van der Ent M, et al. Prospective identification of a large lipid core coronary plaque with a novel near-infrared spectroscopy and intravascular ultrasound (NIR-IVUS) catheter: infarction following stenting possibly due to distal embolization of plaque contents. *J Am Coll Cardiol.* 2010;56:314.
21. Raghunathan D, Abdel-Karim AR, Papayannis AC, et al. Relation between the presence and extent of coronary lipid core plaques detected by near-infrared spectroscopy with postpercutaneous coronary intervention myocardial infarction. *Am J Cardiol.* 2011;107:1613-8.
22. Goldstein JA, Maini B, Dixon SR, et al. Detection of lipid-core plaques by intracoronary near-infrared spectroscopy identifies high risk of periprocedural myocardial infarction. *Circ Cardiovasc Interv.* 2011;4:429-37.
23. Fernandez-Friera L, Garcia-Alvarez A, Romero A, et al. Lipid-rich obstructive coronary lesions is plaque characterization any important? *JACC Cardiovasc Imaging.* 2010;3:893-5.
24. Porto I, Di Vito L, Burzotta F, et al. Predictors of periprocedural (Type IVa) myocardial infarction, as assessed by frequency-domain optical coherence tomography. *Circ Cardiovasc Interv.* 2012;5:89-96.
25. Hong YJ, Jeong MH, Choi YH, et al. Impact of plaque components on no-reflow phenomenon after stent deployment in patients with acute coronary syndrome: a virtual histology-intravascular ultrasound analysis. *Eur Heart J.* 2011;32:2059-66.
26. Pu J, Mintz GS, Brilakis ES, et al. In vivo characterization of coronary plaques: novel findings from comparing greyscale and virtual histology intravascular ultrasound and near-infrared spectroscopy. *Eur Heart J.* 2012;33:372-83.
27. Madder RD, Smith JL, Dixon SR, Goldstein JA. Composition of target lesions by near-infrared spectroscopy in patients with acute coronary syndrome versus stable angina. *Circ Cardiovasc Interv.* 2012;5:55-61.
28. Wood FO, Badhey N, Garcia B, et al. Analysis of saphenous vein graft lesion composition using near-infrared spectroscopy and intravascular ultrasonography with virtual histology. *Atherosclerosis.* 2010;212:528-33.
29. Hong MK, Mehran R, Dangas G, et al. Creatine kinase-MB enzyme elevation following successful saphenous vein graft intervention is associated with late mortality. *Circulation.* 1999;100:2400-5.
30. Sdringola S, Assali AR, Ghani M, et al. Risk assessment of slow or no-reflow phenomenon in aortocoronary vein graft percutaneous intervention. *Catheter Cardiovasc Interv.* 2001;54:318-24.
31. Selvanayagam JB, Porto I, Channon K, et al. Troponin elevation after percutaneous coronary intervention directly represents the extent of irreversible myocardial injury: insights from cardiovascular magnetic resonance imaging. *Circulation.* 2005;111:1027-32.
32. Brilakis ES, Abdel-Karim AR, Papayannis AC, et al. Embolic protection device utilization during stenting of native coronary artery lesions with large lipid core plaques as detected by near-infrared spectroscopy. *Catheter Cardiovasc Interv.* 2012;80(7):1157-62.
33. Garcia BA, Wood F, Cipher D, Banerjee S, Brilakis ES. Reproducibility of near-infrared spectroscopy for the detection of lipid core coronary plaques and

- observed changes after coronary stent implantation. *Catheter Cardiovasc Interv.* 2010;76:359–65.
34. Papayannis AC, Abdel-Karim AR, Mahmood A, Michael TT, Banerjee S, Brilakis ES. Association of coronary lipid core plaque with intra-stent thrombus formation: a near-infrared spectroscopy and optical coherence tomography study. *Catheter Cardiovasc Interv.* 2013;81(3):488–93.
 35. Reininger AJ, Bernlochner I, Penz SM, et al. A 2-step mechanism of arterial thrombus formation induced by human atherosclerotic plaques. *J Am Coll Cardiol.* 2010;55:1147–58.
 36. Banerjee S, Brilakis ES. Embolic protection during saphenous vein graft interventions. *J Invasive Cardiol.* 2009;21:415–7.
 37. Dixon SR, Grines CL, Munir A, et al. Analysis of target lesion length before coronary artery stenting using angiography and near-infrared spectroscopy versus angiography alone. *Am J Cardiol.* 2012;109:60–6.
 38. Farb A, Burke AP, Kolodgie FD, Virmani R. Pathological mechanisms of fatal late coronary stent thrombosis in humans. *Circulation.* 2003;108:1701–6.
 39. Sakhuja R, Suh WM, Jaffer FA, Jang IK. Residual thrombogenic substrate after rupture of a lipid-rich plaque: possible mechanism of acute stent thrombosis? *Circulation.* 2010;122:2349–50.
 40. Muller JE, Abela GS, Nesto RW, Tofler GH. Triggers, acute risk factors and vulnerable plaques: the lexicon of a new frontier. *J Am Coll Cardiol.* 1994;23:809–13.
 41. Naghavi M, Libby P, Falk E, et al. From vulnerable plaque to vulnerable patient: a call for new definitions and risk assessment strategies: Part II. *Circulation.* 2003;108:1772–8.
 42. Naghavi M, Libby P, Falk E, et al. From vulnerable plaque to vulnerable patient: a call for new definitions and risk assessment strategies: Part I. *Circulation.* 2003;108:1664–72.
 43. Rodes-Cabau J, Bertrand OF, Larose E, et al. Comparison of plaque sealing with paclitaxel-eluting stents versus medical therapy for the treatment of moderate nonsignificant saphenous vein graft lesions. the moderate vein graft lesion stenting with the taxus stent and intravascular ultrasound (VELETI) pilot trial. *Circulation.* 2009;120:1978–86.
 44. Stone GW, Maehara A, Lansky AJ, et al. A prospective natural-history study of coronary atherosclerosis. *N Engl J Med.* 2011;364:226–35.
 45. Muller JE, Tawakol A, Kathiresan S, Narula J. New opportunities for identification and reduction of coronary risk: treatment of vulnerable patients, arteries, and plaques. *J Am Coll Cardiol.* 2006;47:C2–6.
 46. Brugaletta S, Garcia-Garcia HM, Serruys PW, et al. NIRS and IVUS for characterization of atherosclerosis in patients undergoing coronary angiography. *JACC Cardiovasc Imaging.* 2011;4:647–55.
 47. Heo JH, Garcia-Garcia HM, Brugaletta S, et al. Lipid core burden index and Framingham score: can a Systemic Risk Score predict lipid core burden in non-culprit coronary artery? *Int J Cardiol.* 2012;156:211–3.
 48. Simsek C, Garcia-Garcia HM, Brugaletta S, et al. Correlation between kidney function and near-infrared spectroscopy derived lipid-core burden index score of a non-intervened coronary artery segment. *Int J Cardiol.* 2012;156:226–8.
 49. Zynda TK, Thompson CD, Seto AH, et al. Evaluation of Coronary Arterial Lipid Content with Angiographic Complexity: Comparison of Near-Infrared Spectroscopy and SYNTAX Score. *Catheter Cardiovasc Interv.* 2011;77:S1–110.
 50. Sacks FM, Rudel LL, Conner A, et al. Selective delipidation of plasma HDL enhances reverse cholesterol transport in vivo. *J Lipid Res.* 2009;50:894–907.
 51. Bose D, von Birgelen C, Erbel R. Intravascular ultrasound for the evaluation of therapies targeting coronary atherosclerosis. *J Am Coll Cardiol.* 2007;49:925–32.
 52. Abdel-Karim AR, Rangan BV, Banerjee S, Brilakis ES. Intercatheter reproducibility of near-infrared spectroscopy for the in vivo detection of coronary lipid core plaques. *Catheter Cardiovasc Interv.* 2011;77:657–61.